Rare Met. (2017) 36(4):229–235
DOI 10.1007/s12598-016-0791-7

RARE METALS
www.editorialmanager.com/rmet

Controlled growth of Au/Ni bimetallic nanocrystals with different nanostructures

Si-Bin Duan, Rong-Ming Wang*

Received: 5 May 2016 / Revised: 13 June 2016 / Accepted: 15 June 2016 / Published online: 1 July 2016

Abstract Bimetallic nanomaterials are of great significance to both fundamental research and industrial applications. Their physicochemical performances are critically dependent on their architectures and electronic structures. Here, it was reported a controlled synthesis of Au/Ni bimetallic nanocrystals with different nanostructures, i.e., dumbbell, core@shell and alloyed nanostructures in a one-pot synthesis procedure. Detailed structural characterizations were conducted with the combination of transmission electron microscopy (TEM) and X-ray diffraction (XRD). Even there is a large lattice mismatch between Au and Ni, Au@Ni core@shell nanocrystals are obtained with the seeded growth method. The growth mechanism was deeply investigated. Triphenylphosphine is demonstrated to be an effective capping agent to modify the interfacial energy to form core@shell nanocrystals, and the higher temperature is proved to be a key role in obtaining alloyed nanocrystals.

Keywords Bimetallic nanomaterials; Au/Ni nanocrystals; Interfacial energy; Core@shell structure

1 Introduction

With the increasing requirement for new materials caused by rapid progress in microelectronics [1, 2], probing technique [3, 4] and life science [5, 6], nanoscience has been developed into a dominant technology [7–9]. Since single-component nanomaterials cannot meet the practical demands to some extent, research into binary materials with specific nanostructures has attracted much interest [10–12].

Bimetallic nanocrystals (NCs), composed of noble and magnetic metal elements, perform not only a simple combination of the properties associated with two different metals, but also many interesting and surprising properties [13–18]. Gu et al. have confirmed that Au@Co and Au@Ni bimetallic NCs dispersed on a glassy carbon electrode surface exhibited high surface-enhanced Raman scattering effect for the adsorbed pyridine [19]. The originally low surface enhancement of the Co and Ni could be substantially improved, giving total enhancement factors up to $1 \times 10^3 - 1 \times 10^4$. Yu et al. synthesized hydrophilic Co@Au bimetallic NCs and confirmed that these multifunctional bimetallic NCs could be employed as biocompatible non-viral gene transport vehicles, and induced the intracellular expression of plasmid enhanced green fluorescent protein (pEGFP) [20]. It has also been confirmed that the better catalytic performances of NiPt hollow spheres with an ultrathin shell toward methanol oxidation reaction compared to NiPt solid nanospheres and Pt/C commercial catalyst [21, 22].

Up to now, various methods have been developed for the preparation of magnetic-noble bimetallic nanoparticles, and wet-chemical method has been demonstrated as an efficient process for the synthesis of bimetallic NCs due to its low cost, low energy consumption and high yield [23, 24]. Vasquez et al. [25] reported a one-pot synthetic strategy for accessing hollow CoPt alloyed nanospheres, utilizing an in situ Co template and exploiting galvanic displacement reaction to selectively dissolve the Co core while depositing a Pt shell. Tsuji et al. [26] adopted epitaxial growth process to control Ni shell formed on the surface of pre-synthesized Au nanoparticles, forming Au@Ni core@shell NCs.

S.-B. Duan, R.-M. Wang*
School of Mathematics and Physics, University of Science and Technology Beijing, Beijing 100083, China
e-mail: rmwang@ustb.edu.cn

However, owing to the large lattice mismatch (~16 %) between magnetic Ni and noble Au metals, which causes large surface tension, little work has been devoted into Au/Ni system [27–30], especially research into Au/Ni NCs with different nanostructures (dumbbell, core@shell and alloyed) produced in a specified synthesis system. Au/Ni bimetallic NCs, especially with core@shell NCs, have been proved to exhibit excellent performances in the fields of optical [19, 26], magnetic [29, 31] and catalytic [32, 33] applications, and thus, it is essential to synthesize Au/Ni bimetallic NCs with different architectures, understand their growth mechanism and investigate the relationship between their nanostructures and physicochemical properties deeply.

In this work, it was focused on the preparation and characterization of three kinds of Au/Ni NCs, i.e., Au–Ni dumbbell, Au@Ni core@shell and AuNi alloyed NCs. A one-pot seeded growth method was developed. By changing simple thermodynamic factors during the synthesis process, i.e., the temperature and the addition of capping agent, three kinds of NCs can be obtained, and the growth mechanism was discussed in detail.

2 Experimental

2.1 Chemicals

Nickel(II) acetylacetonate ($Ni(acac)_2$, 97.0 %), chloroauric acid ($HAuCl_4{\cdot}4H_2O$, 99.0 %), oleylamine (OAm, 98.0 %), triphenylphosphine (TPP, 99.0 %), trioctylphosphine oxide (TOPO, 98.0 %), acetone (99.5 %) and toluene (99.5 %) were all purchased from Chinese Reagent Companies. All reagents were analytic grade and used as-received without further purification.

2.2 Synthesis of Au/Ni bimetallic NCs

2.2.1 Au–Ni dumbbell NCs

In a typical synthesis, $Ni(acac)_2$ (0.5 g) was dissolved in 10 ml OAm and then heated up to 100 °C for 15 min, forming a blue-green solution. A freshly prepared solution of $HAuCl_4{\cdot}4H_2O$ (0.05 g in 5 ml of toluene) was then added dropwise with vigorous stirring and kept at 100 °C for 60 min. Then, the mixed solution was heated to 230 °C for 60 min and naturally cooled to room temperature. The product was collected by centrifugation and washed several times with acetone.

2.2.2 Au@Ni core@shell NCs

In a typical synthesis, $Ni(acac)_2$ (0.5 g) was dissolved in 10 ml OAm and then heated up to 100 °C for 15 min. A freshly prepared solution of $HAuCl_4{\cdot}4H_2O$ (0.02 g in 2 ml of toluene) was then added dropwise with stirring and kept at 100 °C for 60 min. TPP (1.0 g) was added to the mixed solution, and then, the mixed solution was heated to 230 °C for 60 min. The solution was naturally cooled to room temperature before the product was collected by centrifugation and washed several times with acetone.

2.2.3 AuNi alloyed NCs

In a typical synthesis, $Ni(acac)_2$ (0.5 g) was dissolved in 10 ml OAm and then heated up to 100 °C for 15 min. A freshly prepared solution of $HAuCl_4{\cdot}4H_2O$ (0.05 g in 5 ml of toluene) was then added dropwise with stirring and kept at 100 °C for 60 min. Then, the mixed solution was heated to 270 °C for 60 min and naturally cooled to room temperature. The product was collected by centrifugation and washed several times with acetone.

2.2.4 Au/Ni oligomer-like NCs

In a typical synthesis, $Ni(acac)_2$ (0.5 g) was dissolved in 10 ml OAm and then heated up to 100 °C for 15 min. A freshly prepared solution of $HAuCl_4{\cdot}4H_2O$ (0.02 g in 2 ml of toluene) was then added dropwise with stirring and kept at 100 °C for 60 min. TOPO (1.0 g) was added to the mixed solution, and then, the mixed solution was heated to 230 °C for 60 min. The product was collected by centrifugation and washed several times with acetone.

2.3 Materials characterization

The crystal structures, morphologies and chemical compositions of the as-prepared products were studied using X-ray diffractometer (XRD, X'Pert Pro MPD system) with Cu Kα and $\lambda = 0.15409$ nm and transmission electron microscopy (TEM, JEOL 2100F) with field emission gun and accelerating voltage of 200 kV. For the XRD measurements, powder samples dried in a vacuum oven were used. The specimen for TEM investigation was prepared by dispersing the powder products in toluene by ultrasonic treatment and then dropped onto a porous carbon film supported on a copper grid and dried in a vacuum oven.

3 Results and discussion

3.1 Morphological and structural characterization

The as-synthesized materials were first identified as Au/Ni bimetallic NCs with different architectures. High-resolution TEM (HRTEM) image (Fig. 1a) shows the dumbbell morphology of an Au–Ni NC, which has a ~5 nm Au-riched tip and a ~10 nm Ni-riched tail. As Fig. 1b shows,

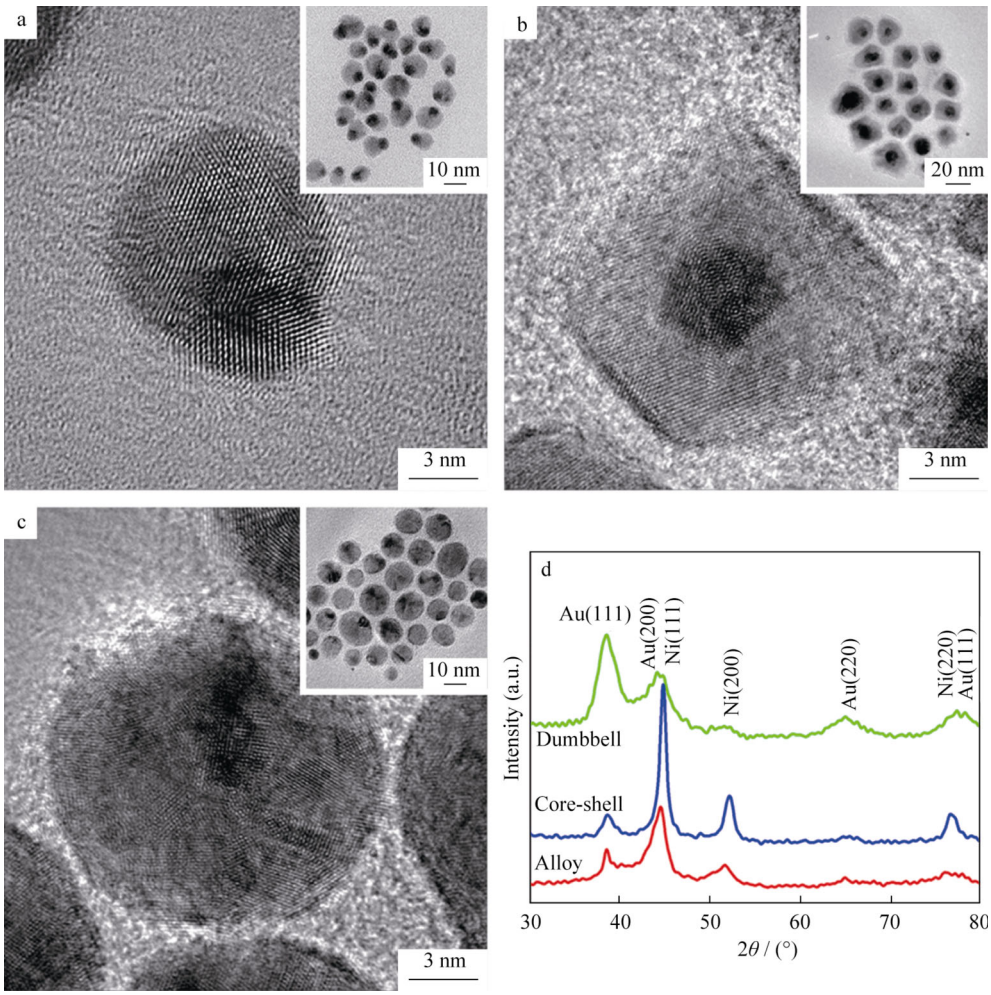

Fig. 1 HRTEM images of Au/Ni bimetallic NCs: **a** dumbbell, **b** core@shell and **c** alloyed (insets being corresponding low-magnified bright TEM images); **d** XRD patterns of Au/Ni bimetallic NCs

the darker core and the brighter shell suggest the formation of core@shell nanostructure with a core diameter of ~4 nm and a shell thickness of ~5 nm in an Au@Ni NC; especially, HRTEM image suggests that the outer Ni shell exhibits single-crystalline nature, which is different from the reported epitaxially grown Au@Ni NCs in ethylene glycol [27]. Figure 1c shows a typical HRTEM image for a particular NC synthesized at high temperature, where no obvious interface between Au and Ni is observed, demonstrating the formation of alloyed structure with the mean diameter of ~15 nm. The low-magnified TEM images of these three kinds of NCs are shown in the insets, indicating that all of the three Au/Ni NCs with different nanostructures exhibit structural purity.

To confirm the crystal nature, XRD characterization was conducted. As shown in Fig. 1d, the peaks of the XRD patterns can be attributed to fcc Au phase (JCPDF No. 04-0784) and fcc Ni phase (JCPDF No. 04-0850). The Ni peak heights of Au@Ni core@shell NCs are obviously higher, resulting from the good crystallization rate and coinciding with the single-crystal shell nature from the TEM results. Broadening of the XRD peaks may result from the small grain sizes, of which core@shell NCs are estimated to be ~5.7 nm for Au using (111) peak and ~9.8 nm for Ni using (200) peak by Scherrer's equation:

$$d = 0.89\lambda/\beta\cos\theta_B \quad (1)$$

where d is grain size, $\lambda = 0.15406$ nm is the X-ray wavelength, θ_B is the Bragg diffraction angle and β is the peak full width at half maximum. And the grain sizes of Au–Ni dumbbell NCs are estimated to be ~8.1 nm for Au and ~4.1 nm for Ni. The shift of XRD peak positions confirms the alloyed nature of the AuNi alloyed NCs accordingly.

3.2 Growth mechanism

Because of the large lattice mismatch between Au and Ni, it is difficult to control the nanostructure of Au/Ni bimetallic NCs, especially to form a core@shell

nanostructure with a single-crystal shell. Understanding the growth mechanism is critically important and can provide more insight into a new synthesis method for other types of bimetallic nanomaterials. To better understand the growth mechanism, contrast experiments were conducted and several thermodynamic parameters were highlighted.

3.2.1 Au–Ni dumbbell NCs

For the synthesis of dumbbell-like nanostructure, it is essential to control the growth of the second component under the island growth model on the surfaces of preformed seeds [34]. In the synthesis of Au/Ni bimetallic NCs, the Au nanoparticles were first obtained at 100 °C with the reduction $HAuCl_4$ by OAm because of the higher redox potential of Au than that of Ni. The resultant Au NCs exhibit icosahedral shape and serve as seeds in the second step to deposit Ni atoms on their surfaces at 230 °C. Because of the large lattice mismatch between Au and Ni and the small size effect, which induce large lattice strain and high interfacial energy, the Ni atoms prefer to grow according to the island growth model, thus forming the dumbbell-like nanostructure to balance the ultimate Gibbs free energy.

3.2.2 Au@Ni core@shell NCs

For Au/Ni bimetallic NCs, it is difficult to form core@shell NCs through the traditional seeded growth method since the high interfacial energy results from the large lattice mismatch between Au and Ni elements. As above, Au–Ni dumbbell NCs are obtained without the addition of TPP. When TPP was added into the synthesis solution containing the preformed Au seeds at 100 °C, the samples are considered as Au@Ni core@shell NCs. In order to confirm their core@shell structural nature further, angle-dependent HRTEM characterization was conducted from various viewing angles. As shown in Fig. 2, by observing a particular NC from different view angles, the darker Au is all positioned in the core region, further verifying the core@shell structural nature of the product.

It is obvious that TPP plays an important role in the growth of Ni atoms on the surface of Au seeds under the layered growth model. TPP has been proved to be an effective capping agent for Au atoms [35]. Thus, TPP can be tightly bound to the surface atoms of Au nanoparticles during the deposition of Ni atoms. The capping effect of TPP could reduce the interfacial energy, thus favor the layer growth and induce the core@shell structure formation. However, TPP is also an effective phosphorus source

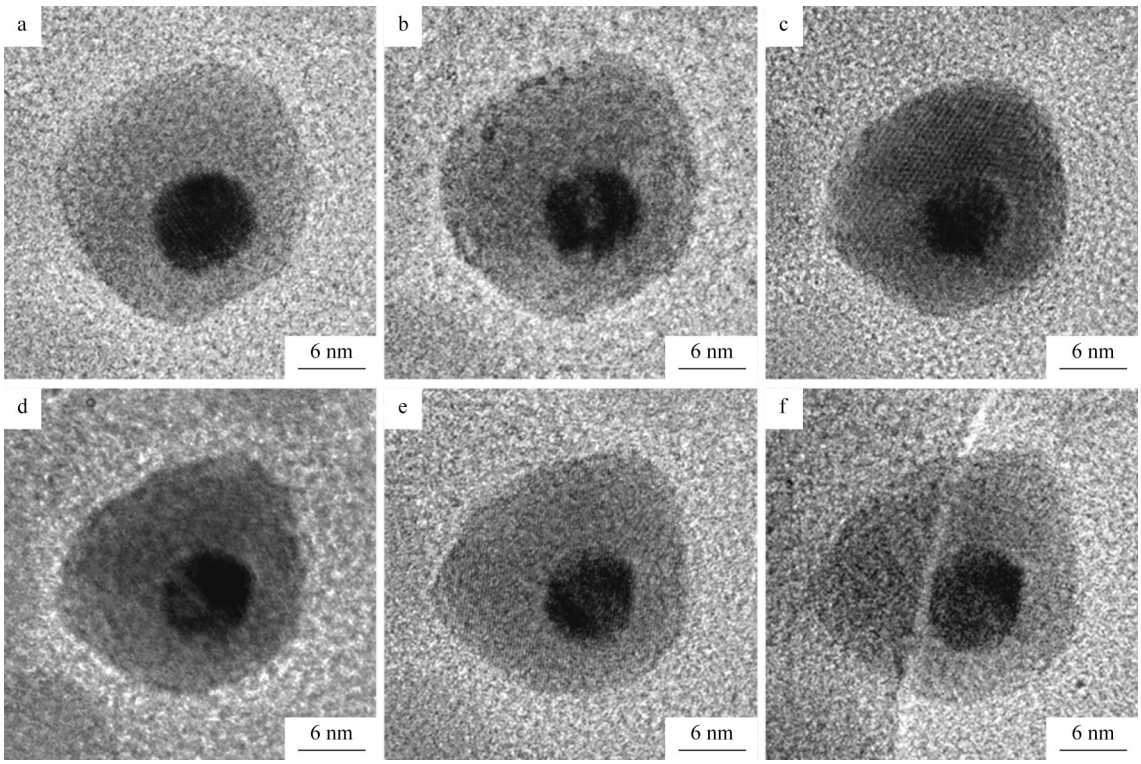

Fig. 2 HRTEM images of an Au@Ni core@shell NC from different view angles: **a** 30°, **b** 20°, **c** 10°, **d** 0°, **e** −10° and **f** −20° (providing a certain proof for core@shell architecture rather than upright dumbbells)

for Ni and can transform Ni to nickel phosphide, and it has been previously confirmed that Au@$Ni_{12}P_5$ core@shell NCs are obtained when the synthesis temperature is raised to 270 °C with the addition of TPP [35]. However, if the synthesis temperature is reduced to below 180 °C, no nickel could be obtained, due to the fact that the reduction of Ni by OAm needs higher temperature (230 °C) here. Thus, the temperature control is essential to obtain Au@Ni core@shell NCs. Besides, the adding order of TPP is critically important. When adding TPP before the addition of $HAuCl_4$, no Au nanoparticle is obtained, which is also resulting from the strong capping effect of TPP. When adding TPP after the formation of Au–Ni dumbbell NCs, the morphology of Au–Ni NCs is retained, demonstrating that Au–Ni dumbbell NCs are quiet stable at 230 °C as long as they are formed in the OAm.

In addition, the choice of capping agent was also investigated. When the TPP was replaced by TOPO, oligomer-like Au/Ni NCs were fabricated, as shown in Fig. 3. The Au nanoparticles are attached by several Ni nanoparticles, different from the core@shell NCs, where the Au cores are evenly embedded within Ni shells. The oligomer-like nanostructure is also different from the dumbbell-like one, where the Au and Ni nanoparticles are attached to each other. This is mainly because that the capping effect of TOPO on Au atoms is not as strong as that of TPP, resulting from the lack of unshared electrons in the P atoms in TOPO with P=O bonding. Thus, the TOPO-capped Au nanoparticles will serve several growth sites for Ni atoms and more than one Ni nanoparticles grow on the Au surface, forming oligomer-like Au–Ni NCs ultimately.

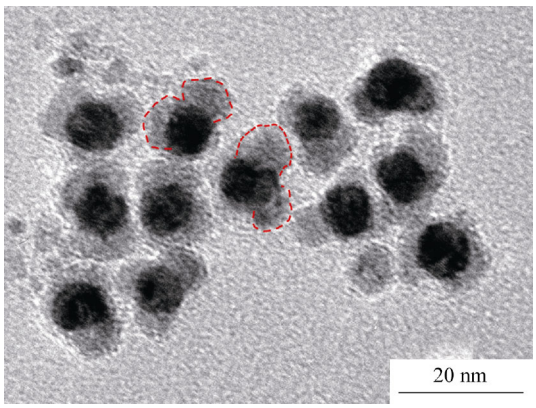

Fig. 3 TEM image of Au/Ni oligomer-like Au/Ni NCs synthesized with the addition of TOPO at 230 °C (dotted line showing outer shape of Ni NCs)

3.2.3 AuNi alloyed NCs

During the formation of AuNi alloyed NCs, the effect of temperature was highlighted. When the synthesis temperature increases to 270 °C, alloyed NCs are obtained through the random aggregation of bimetallic crystallites. It also demonstrates that the Au atoms migrate under higher temperature, which was previously proved using in situ scanning transmission electron microscopy [36]. In addition, it is also confirmed that when raising the temperature of OAm containing Au–Ni dumbbell or Au@Ni core@shell NCs, the AuNi alloyed NCs could also be obtained, suggesting that Au and Ni atoms will migrate at

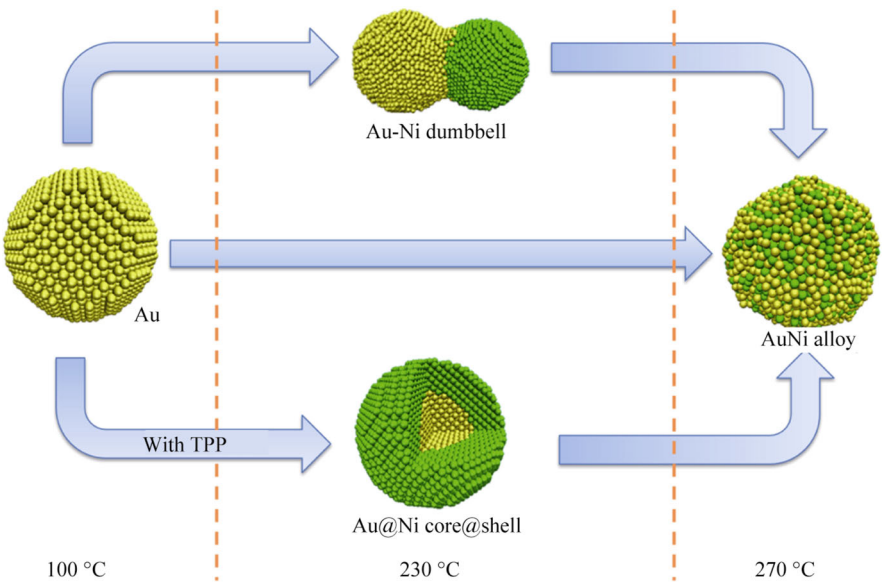

Fig. 4 Schematic illustration of formation of Au/Ni bimetallic NCs

high temperature and AuNi alloyed nanostructure is energetic preferred at 270 °C.

In summary, the growth mechanism of Au/Ni bimetallic is shown in Fig. 4. At 100 °C, Au NCs are obtained and serve as seeds to deposit Ni atoms on their surfaces. At 230 °C, the large lattice mismatch induces the island growth model and thus gives rise to the formation of Au–Ni dumbbell NCs. During this procedure, the usage of TPP can efficiently reduce the interfacial energy and thus benefit the formation of Au@Ni core@shell NCs. At higher temperature, 270 °C here, Au and Ni atoms will migrate to form AuNi alloyed NCs.

4 Conclusion

In conclusion, it is demonstrated that Au and Ni can form bimetallic NCs with three kinds of nanostructures, i.e., dumbbell, core@shell and alloyed, in a simple procedure. TEM and XRD characterizations confirm their structures and morphologies. Series of experiments demonstrate that controlling the interfacial energy by the addition of TPP can help to form Au@Ni core@shell NCs under layered growth model. The high temperature is the key factor to producing the alloyed AuNi NCs. As the properties of nanomaterials critically depend on their nanostructures, it is believed that the AuNi bimetallic NCs with different nanostructures synthesized in this work can act as promising catalytic and magnetic materials based on their structural properties.

Acknowledgments This study was financially supported by the National Natural Science Foundation of China (Nos. 51371015 and 51331002), Beijing Municipal Research Project for Outstanding Doctoral Thesis Supervisors (No. 20121000603), Beijing Natural Science Foundation (No. 2142018) and the Fundamental Research Funds for the Central Universities (No. FRF-BR-15-009B).

References

[1] Choi JH, Wang H, Oh SJ, Paik T, Sung P, Sung J, Ye X, Zhao T, Diroll BT, Murray CB, Kagan CR. Exploiting the colloidal nanocrystal library to construct electronic devices. Science. 2016;352(6282):205.
[2] Sashchiuk A, Yanover D, Rubin-Brusilovski A, Maikov GI, Capek RK, Vaxenburg R, Tilchin J, Zaiats G, Lifshitz E. Tuning of electronic properties in IV–VI colloidal nanostructures by alloy composition and architecture. Nanoscale. 2013;5(17):7724.
[3] Raja SN, Olson AC, Thorkelsson K, Luong AJ, Hsueh L, Chang G, Gludovatz B, Lin L, Xu T, Ritchie RO, Alivisatos AP. Tetrapod nanocrystals as fluorescent stress probes of electrospun nanocomposites. Nano Lett. 2013;13(8):3915.
[4] Wang Y, Yan B, Chen L. SERS tags: novel optical nanoprobes for bioanalysis. Chem Rev. 2013;113(3):1391.
[5] Lee YK, Lee H, Nam JM. Lipid-nanostructure hybrids and their applications in nanobiotechnology. NPG Asia Mater. 2013;5(5):e48.
[6] Domling A, Wang W, Wang K. Chemistry and biology of multicomponent reactions. Chem Rev. 2012;112(6):3083.
[7] Ibanez M, Cabot A. Chemistry. All change for nanocrystals. Science. 2013;340(6135):935.
[8] Zhang LB, Wang EK. Metal nanoclusters: new fluorescent probes for sensors and bioimaging. Nano Today. 2014;9(1):132.
[9] Kumaraswamy G, Kumar S, Kulkarni S, Srivastav A, Roy Chowdhury P, Pavan Kumar GV, Eiser E, Edwards A, Prasad BL, Basavaraj MG, Shetti N, Bockstaller M, Medhi H, Joshi YM, John NS, Chakravarty C, Shinde V, Bandyopadhyaya R, Kotov N, Krishnamoorti R, Couty M, Jestin J, Frenkel D. Nanocomposites: general discussion. Faraday Discuss. 2016;186:277.
[10] Duan S, Wang R. Bimetallic nanostructures with magnetic and noble metals and their physicochemical applications. Prog Nat Sci Mater. 2013;23(2):113.
[11] Xu ML, Yang XK, Zhang YJ, Xia SB, Dong P, Yang GT. Enhanced methanol oxidation activity of Au@Pd nanoparticles supported on MWCNTs functionalized by MB under ultraviolet irradiation. Rare Met. 2015;34(1):12.
[12] Sankar M, Dimitratos N, Miedziak PJ, Wells PP, Kiely CJ, Hutchings GJ. Designing bimetallic catalysts for a green and sustainable future. Chem Soc Rev. 2012;41(24):8099.
[13] Sun X, Li D, Ding Y, Zhu W, Guo S, Wang ZL, Sun S. Core/shell Au/CuPt nanoparticles and their dual electrocatalysis for both reduction and oxidation reactions. J Am Chem Soc. 2014;136(15):5745.
[14] Hsia C-F, Madasu M, Huang MH. Aqueous phase synthesis of Au–Cu core–shell nanocubes and octahedra with tunable sizes and noncentrally located cores. Chem Mater. 2016;28(9):3073.
[15] Zhang Y, Wang Q, Ashall B, Zerulla D, Lee GU. Magnetic-plasmonic dual modulated FePt–Au ternary heterostructured nanorods as a promising nano-bioprobe. Adv Mater. 2012;24(18):2485.
[16] Ataee-Esfahani H, Wang L, Nemoto Y, Yamauchi Y. Synthesis of bimetallic Au@Pt nanoparticles with Au core and nanostructured Pt shell toward highly active electrocatalysts. Chem Mater. 2010;22(23):6310.
[17] Zheng X, Guo YL, Guo Y, Zhang Q, Liu XH, Wang L, Zhan WC, Lu GZ. Epoxidation of propylene by molecular oxygen over unsupported $AgCu_x$ bimetallic catalyst. Rare Met. 2015;34(7):477.
[18] Wang L, Nemoto Y, Yamauchi Y. Direct synthesis of spatially-controlled Pt-on-Pd bimetallic nanodendrites with superior electrocatalytic activity. J Am Chem Soc. 2011;133(25):9674.
[19] Bao F, Li JF, Ren B, Gu RA, Tian ZQ. Synthesis and characterization of Au@Co and Au@Ni core−shell nanoparticles and their applications in surface-enhanced raman spectroscopy. J Phys Chem C. 2008;112(2):345.
[20] Lu Y, Zhao Y, Yu L, Dong L, Shi C, Hu MJ, Xu YJ, Wen LP, Yu SH. Hydrophilic Co@Au yolk/shell nanospheres: synthesis, assembly, and application to gene delivery. Adv Mater. 2010;22(12):1407.
[21] Sun Q, Ren Z, Wang R, Wang N, Cao X. Platinum catalyzed growth of NiPt hollow spheres with an ultrathin shell. J Mater Chem. 2011;21(6):1925.
[22] Shan AX, Cheng M, Fan HS, Chen ZC, Wang RM, Chen CP. NiPt hollow nanocatalyst: green synthesis, size control and electrocatalysis. Prog Nat Sci Mater. 2014;24(2):175.
[23] Liao H, Fisher A, Xu ZJ. Surface segregation in bimetallic nanoparticles: a critical issue in electrocatalyst engineering. Small. 2015;11(27):3221.

[24] Wei S, Wang Q, Zhu J, Sun L, Lin H, Guo Z. Multifunctional composite core-shell nanoparticles. Nanoscale. 2011;3(11): 4474.
[25] Vasquez Y, Sra AK, Schaak RE. One-pot synthesis of hollow superparamagnetic CoPt nanospheres. J Am Chem Soc. 2005; 127(36):12504.
[26] Tsuji M, Yamaguchi D, Matsunaga M, Ikedo K. Epitaxial growth of Au@Ni core − shell nanocrystals prepared using a two-step reduction method. Cryst Growth Des. 2011;11(5): 1995.
[27] Huang L, Shan A, Li Z, Chen C, Wang R. Phase formation, magnetic and optical properties of epitaxially grown icosahedral Au@Ni nanoparticles with ultrathin shells. Cryst Eng Comm. 2013;15(13):2527.
[28] Wang D, Schaaf P. Ni–Au bi-metallic nanoparticles formed via dewetting. Mater Lett. 2012;70:30.
[29] She HD, Chen YZ, Chen XZ, Zhang K, Wang ZY, Peng DL. Structure, optical and magnetic properties of Ni@Au and Au@Ni nanoparticles synthesized via non-aqueous approaches. J Mater Chem. 2012;22(6):2757.
[30] Zhong S, Duan S, Cui Y. Electrode dependence of resistive switching in Au/Ni–Au nanoparticle devices. RSC Adv. 2014; 4(77):40924.
[31] Chiang IC, Chen YT, Chen DH. Synthesis of NiAu colloidal nanocrystals with kinetically tunable properties. J Alloys Compd. 2009;468(1–2):237.
[32] Song JH, Yu JY, Zhang MZ, Liang YJ, Xu CW. Glycerol electrooxidation on Au/Ni core/shell three-dimensional structure catalyst. Int J Electrochem Sci. 2012;7(5):4362.
[33] Molenbroek AM, Norskov JK, Clausen BS. Structure and reactivity of Ni–Au nanoparticle catalysts. J Phys Chem B. 2001;105(23):5450.
[34] Carbone L, Cozzoli PD. Colloidal heterostructured nanocrystals: synthesis and growth mechanisms. Nano Today. 2010;5(5):449.
[35] Duan SB, Wang RM. Au/$Ni_{12}P_5$ core/shell nanocrystals from bimetallic heterostructures: in situ synthesis, evolution and supercapacitor properties. NPG Asia Mater. 2014;6:e122.
[36] Liu W, Sun K, Wang RM. In situ atom-resolved tracing of element diffusion in NiAu nanospindles. Nanoscale. 2013;5(11): 5067.